Penerbit Akademia Baru

Journal of Advanced Research in Experimental Fluid Mechanics and Heat Transfer

http://www.akademiabaru.com/submit/index.php/arefmht

ISSN: 2756-8202

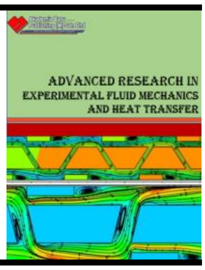

Impacts of Nonlinear Thermal Radiation on a Stagnation Point of an Aligned MHD Casson Nanofluid Flow with Thompson and Troian Slip Boundary Condition

T. W. Akaje[1,*], B. I Olajuwon[2]

[1] Department of Mathematics, Federal University of Agriculture, Abeokuta, Nigeria
[2] Department of Mathematics, Federal University of Agriculture, Abeokuta, Ogun State, Nigeria

ABSTRACT

This paper investigates the impact of the nonlinear radiative heat on the species heat transfer of a MHD Casson nanofluid flow with stagnation point associated with Thompson and Troian boundary conditions. In the study, the flow system is considered in a Dacry-Forchheimmer porous media in the presence of combination nonlinear thermal radiation and Thompson and Troian slip boundary conditions. With the aid of suitable transformation quantities, the governing appropriate model for the physical phenomenon is transformed into a dimensionless equation, and solutions are obtained numerically by employing the spectral collocation method. The influences of pertinent fluid physical terms on the thermal and species transfer of a MHD Casson nanoliquid are carefully studied. The qualitative outcomes on the investigation are reported in graphs and in tabular form. A comparative study of earlier results is made with the present and a quantitative agreement is found. The skin friction, local Nusselt number and local Sherwood number are as well analysed and the outcomes are offered in the table. The results reveal that the enhancement of the thermal relaxation parameter reduced the temperature of the fluid. Furthermore, the temperature is increased when temperature ratio, thermal radiation, Biot number, Eckert number, and Casson parameter are enhanced. Hence, the results are useful in improving thermal science devices and increasing industrial out.

Keywords:
Casson nanofluid; nonlinear thermal radiation; Thompson and Troian slip boundary condition; inclined magnetic field

1. Introduction

The study of boundary layer non-Newtonian fluid flow is more significant now are day than before because of it numerous applications in industries. The Casson fluid model has an exceptional usage in the chemical and biological industries. This fluid model exhibits a yield stress greater than the shear stress that makes it behaves like solids while deformation occur when the yield stress is lesser than the shear stress. Numerous researches have been carried out to inspect the rheological properties of this non-Newtonian Casson fluid. In this view, Gireesha *et. al.*, [1] considered the impact of heat Cattaneo-Christov flux on the dusty Casson liquid flow past an elongating sheet with the influence of melting heat transport. They reported that the melting effect upsurges the temperature distribution for both fluid and dusty phases. A free convective transient stretching sheet flow of Casson fluid and

* *Corresponding author.*
E-mail address: akajewasiu@gmail.com

entropy generation analysis is studied by Mabood *et. al*., [2]. Influence of heat transfer of transient magneto-hydrodynamics Casson fluid with the presence of inclined parallel plates investigated by Kirubhashankar *et. al*., [3]. The results show that the momentum boundary layer viscosity reduced with an increasing in both magnetic field and Prandtl number. Reddy *et. al*., [4] applied implicit finite method to analysis the influence of chemical reaction and slip on the Casson fluid in the presence of heat Cattaneo-Christove flux formulation. It was observed that increase in the inclination angle reduces the flow velocity. Computational analysis of incompressible stagnation boundary layer flow over an extending medium with the occurrence of viscous heat dissipation and magnetic field was studied by AbdEl-Aziz andAfify [5]. Khan *et. al*., [6] examined the effects of heat and flow rate slips on the stagnation point hydromagnetic variable heat reservoir flow past nonlinear stretching device. Casson fluid stagnation point flow past an exponentially expanding plate with Newtonian heating and varying heat conductivity was explored by Ahmad *et. al*., [7]. Imran *et. al*., [8] introduced Keller box method to analyze MHD slip flow of Casson fluid along a nonlinear permeable stretching cylinder saturated in a porous medium with chemical reaction, viscous dissipation, and heat generation/Absorption and the findings proved that, The magnitude of wall shear stress is noticed to be higher with an increase in porosity and suction/blowing parameters. Dual similarity solutions of MHD stagnation point flow of Casson fluid with effect of thermal radiation and viscous dissipation: stability analysis was investigated by Liaquat *et. al*., [9]. Some related investigated concerning the model Casson fluid flow in various geometries can be seen in Refs. [10-11].

In fluid dynamics, radiative heat either nonlinear or linear plays major impact in diverse enormous temperature processes because of it several applications in power plant and industries. The mechanism involving heat transport is highly essential and needed in the industry for final possessions of desired qualities. Modern system connected to space vehicle, power generator plasma, reactor cooling, astrophysical flow and so on are developed based on radiation applications, Uddin *et. al*., [12]. In this regard, Ibukun *et. al*., [13] examined the reaction of Dufour and Soret to an increasing slip velocity, convective boundary and thermal radiation for a fluid flow dynamic, and it was detected that radiation increases the boundary layer viscidness because the system heat transfer is stimulated. Nanofluid radiaitive MHD flow through an exponentially increasing plate in permeable medium was analyzed numerically by Thaigarajan and Kumar [14]. Unsteady conducting radiative chemical reaction nanoliquid flow in a stretching medium on was reviewed by yahaya *et. al*., [15]. Multiple slip effects on MHD non-Newtonian nanofluid flow over a nonlinear permeable elongated sheet was examined by Raza *et. al*.,[16].

Hayat *et. al*., [17] investigated the influences of nonlinear thermal radiation and nanomaterials in minimization dynamical impact of entropy generation on the industrial output. An increasing heat transport rate was found from their results due to rising Biot number that leads to temperature rising while the temperature enhanced with lager value of biot number and temperature ratio. Syed *et. al*., [18] studied thermal transport investigation in magneto-radiative GO-MoS2/H2O-C2H6O2 hybrid nanofluid subject to Cattaneo–Christov model. Khan *et. al*., [19] studied On the Cattaneo–Christov Heat Flux Model and OHAM analysis for three Diferent types of nanofluids, and an important fact is observed when the thermal radiation is increased progressively because there is reduction on temperature field and boundary layer thickness. Eswar and Sreenadh [20] examined the impact of chemical reaction and heat radiation on the steady viscoelastic fluid with convective boundary layer. The findings show that enhancing thermal radiation boosted temperature profile. Kumar *et. al*., [21] considered nonlinear radiation impact and chemical quartic reaction of the nanotubes carbon flow. Hydrodynamic analysis of laminar mixed convective flow of Ag-TiO_2- water hybrid nanofluid in a horizontal annulus was studied by Badr Ali *et. al*., [22]. Mixing Chamber for Preparation of Nanorefrigerant was investigated by Fazlin and Azwadi [23] and the result was showed that mixing chamber design with wall thickness of 10 mm showed the lowest maximum displacement and the maximum von Misses stress does not exceed yield strength of the material. Effects of Solar Radiation and Viscous Dissipation on Mixed Convective Non-Isothermal Hybrid Nanofluid over Moving Thin Needle were carried by Sultana *et. al.*, [24]. Activity of Viscoelastic Nanofluid Film Sprayed on a Stretching Cylinder with Arrhenius Activation Energy and Entropy Generation was examined by Auwalu *et. al.*, [25]. A numerical solution of radiation and Dufour effect on the hydromagnetic non-conducting plate with species reaction was investigated by Vijayaragavan and Karthikeyan [26]. Non-Newtonian MHD heat transfer fluid in porous media over a stretching plate with heat source and linear thermal radiation was inspected by Noura [27]. Convection heat mass transfer and MHD flow over a vertical plate with chemical reaction, arbitrary shear stress and exponential heating was examined by Sehra *et. al.*, [28]. The result show that higher value of Pr number, η1 parameter, Sc number, η_2 parameter and MHD parameter *M* reduce the motion of fluid, while as in the absence of η_1 parameter, η_2 parameter and MHD parameter *M* the motion of fluid is increasing.

In line with the above mentioned literature survey, studies of non-Newtonian fluid flow with a nonlinear slip and radiation effect are limited. However, the usefulness is not limited, this therefore stimulate and motivate the current study with the intention to study the nonlinear thermal radiation effect impinged on a stagnation point of an aligned MHD Casson nanofluid flow with convective and Thompson and Troian slip boundary condition. The outcomes of this sensitivity analysis will be useful to modern technological advancement in enhancing industrial productivity. Furthermore, thermodynamic properties such as viscous dissipation effect and heat source are accounted to capture heat transfer characteristics. The numerical results are obtained using the spectral-collocation method for velocities and temperature profiles. Also, engineering factors of flow such as the drag skin coefficient, heat gradient and Sherwood number are also reported graphs and tables.

2. Mathematical Formulations

This investigation considers heat and mass transport of non-transient hydromagnetic Casson nanoliquid stagnation-point along a horizontal linearly elastic sheet with boundary convection condition and nonlinear heat radiation. Also, the flow is supposed to be a two-dimensional and laminar with analysis of Thomson and Troian boundary condition. As presented in Figure 1, the external flow velocity is taken as $u_w = ax$ while the sheet stretching velocity denotes $u_e = cx$, here a, c are positive constants. It is assumed further that the magnetic field is inclined and placed along the flow direction at an angle ψ while the magnetic field induction is ignored. The viscous dissipation and the heat generation are considered in the reactive mass fluid flow. With boundary layer, the flow, heat and mass model is presented as [1-2].

The isotropic rheological state equation for Casson incompressible flowing fluid is taken as [2]:

$$\tau_{ij} = \begin{cases} \left(\mu_B + \dfrac{p_y}{\sqrt{2\pi}}\right) 2e_{ij}, & \pi > \pi_c \\ \left(\mu_B + \dfrac{p_y}{\sqrt{2\pi_c}}\right) 2e_{ij}, & \pi < \pi_c \end{cases}, \quad e_{ij} = \frac{1}{2}\left(\frac{\partial u_i}{\partial x_j} + \frac{\partial u_j}{\partial x_i}\right) \tag{1}$$

where the yield stress is denoted by p_y, μ_D denotes dynamical non-Newtonian viscosity plastic liquid, $\pi = e_{ij}e_{ij}, e_{ij}$ is the self-deformation component $(i, j)^{th}$ product and π_c represents the non-Newtonian critical value for π.

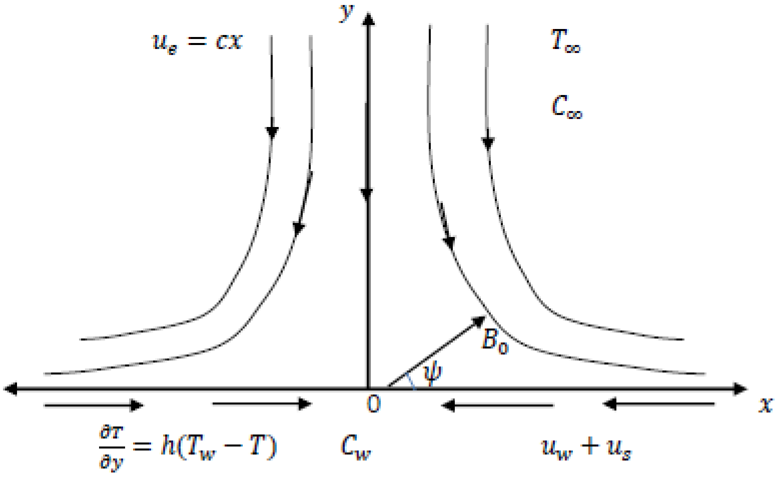

Fig.1. The coordinate flow geometry system

With these assumptions, the systems of differential formulation are presented as [5-7]:

$$\frac{\partial u}{\partial x}+\frac{\partial v}{\partial y}=0 \tag{2}$$

$$u\frac{\partial u}{\partial x}+v\frac{\partial u}{\partial y}=\nu\left(1+\frac{1}{\beta}\right)\frac{\partial^2 u}{\partial y^2}+\frac{\sigma B_o^2\left(u_e-u\right)}{\rho}\sin^2\psi+\frac{\nu\left(u_e-u\right)}{k_0}+Fr\left(u_e^2-u^2\right)+u_e\frac{du_e}{dx} \tag{3}$$

$$u\frac{\partial T}{\partial x}+v\frac{\partial T}{\partial y}=\frac{k}{\rho c_p}\frac{\partial^2 T}{\partial y^2}+\tau\left[D_B\left(\frac{\partial C}{\partial y}\frac{\partial T}{\partial y}\right)+\frac{D_T}{T_\infty}\left(\frac{\partial T}{\partial y}\right)^2\right]+\frac{\mu}{\rho c_p}\left(1+\frac{1}{\beta}\right)\left(\frac{\partial u}{\partial y}\right)^2$$
$$\frac{1}{\rho c_p}\frac{\partial q_r}{\partial y}+\frac{\sigma B_0^2\left(u_e-u\right)^2}{\rho c_p}+\frac{Q_0\left(T-T_\infty\right)}{\rho c_p} \tag{4}$$

$$u\frac{\partial C}{\partial x}+v\frac{\partial C}{\partial y}=D_B\frac{\partial^2 C}{\partial y^2}+\frac{D_T}{T_\infty}\frac{\partial^2 T}{\partial y^2} \tag{5}$$

together with the given appropriate conditions:

$$u=u_w+u_s=\left(1+\frac{1}{\beta}\right)\lambda_1\frac{\partial u}{\partial y}\left(1-\xi_1\frac{\partial u}{\partial y}\right)^{-\frac{1}{2}},\ v=0,\ -k\left(\frac{\partial T}{\partial y}\right)=h\left(T_w-T\right), C=C_\infty \quad \text{at} \quad y=0 \tag{6}$$

$$u\to u_e,\quad T\to T_\infty,\quad C\to C_\infty \quad \text{as} \quad y\to\infty \tag{7}$$

where u and v represent x and y flow rate direction components correspondingly, ρ implies density of the fluid, u_s connotes tangential velocity, ν signifies fluid kinematic viscosity, $\beta=\mu_B\frac{\sqrt{2\pi_c}}{p_y}$ [1] depicts the Casson term, the Navier's slip length is denoted by λ_1 and the reciprocal of some critical shear rate is ξ_1. T_∞ represents temperature of far stream, T_w denotes sheet plate temperature, c_p depicts specific heat, k is the heat conductivity, T is the temperature, σ stand for fluid electrical conductivity, D_B stands for Brownian diffusion coefficient, $\tau=\frac{(\rho c)_p}{(\rho c)_f}$ connotes heat capacity ratio for nanoparticle and the base fluid, D_T denotes coefficient of thermophoretic diffusion, and B_0 represents strength of the inclined magnetic field.

By means of Rosseland's approximation, q_r is defined as

$$q_r = -\frac{4\sigma_s}{3k^*}\frac{\partial T^4}{\partial y} = -\frac{16\sigma_s}{3k^*}T^3\frac{\partial T}{\partial y} \tag{8}$$

in which σ and k^* are respectively the Stefan-Boltzman term and the coefficient absorption mean. Hence, Eq. (4) can be written in the form

$$u\frac{\partial T}{\partial x} + v\frac{\partial T}{\partial y} = \frac{k}{\rho c_p}\frac{\partial^2 T}{\partial y^2} + \tau\left[D_B\left(\frac{\partial C}{\partial y}\frac{\partial T}{\partial y}\right) + \frac{D_T}{T_\infty}\left(\frac{\partial T}{\partial y}\right)^2\right] + \frac{\mu}{\rho c_p}\left(1+\frac{1}{\beta}\right)\left(\frac{\partial u}{\partial y}\right)^2$$
$$\frac{16\sigma_s}{3k\rho c_p}\frac{\partial}{\partial y}\left(T^3\frac{\partial T}{\partial y}\right) + \frac{\sigma B_0^2\left(u_e - u\right)^2}{\rho c_p} + \frac{Q_0\left(T - T_\infty\right)}{\rho c_p} \tag{9}$$

With the aid of the below transformations

$$\eta = \left(\frac{u_w}{\nu x}\right)^{\frac{1}{2}} y,\ \psi(x,y) = \left(u_w \nu\right)^{1/2} x f(\eta),\ \ T = T_\infty\left(1 + (TR-1)\theta(\eta)\right),\ \ \phi(\eta) = \frac{C - C_\infty}{C_w - C_\infty} \tag{10}$$

the function $\psi(x,y)$ represents stream function which is expressed as

$$u = \frac{\partial \psi}{\partial y},\ \ v = -\frac{\partial \psi}{\partial x}$$

The dimensionless model becomes,

$$\left(1+\frac{1}{\beta}\right)f''' + ff'' - f'^2 + A^2 + \left(H\sin\psi + \frac{1}{K}\right)\left(A - f'\right) + Fm\left(A^2 - f'^2\right) \tag{11}$$

$$\frac{1}{Pr}\left(1 + Rt\left(1 + (TR-1)\theta\right)^3\theta'\right)' + f\theta' + N_b\phi'\theta' + N_t\theta'^2 + \left(1+\frac{1}{\beta}\right)Ec\, f''^2$$
$$+ EcH\left(A - f'\right)^2\sin^2\psi + Q\theta = 0 \tag{12}$$

$$\phi'' + Lef\phi' + \frac{N_t}{N_b}\theta'' \tag{13}$$

$$\left.\begin{aligned} &f(0) = 0,\ f'(0) = 1 + \lambda\left(1+\frac{1}{\beta}\right)\frac{\partial u}{\partial y}\left(1 - \xi\frac{\partial u}{\partial y}\right)^{-\frac{1}{2}} f''(0), \theta'(0) = -Bi\left(1 - \theta(0)\right),\ \ \phi(0) = 1 \\ &\qquad f'(\infty) = A,\quad \theta(\infty) = 0,\quad \phi(\infty) = 0 \end{aligned}\right\} \tag{14}$$

The emerging terms in the above mathematical system are defined below as:

$$Pr = \frac{\nu}{\alpha}, Le = \frac{\nu}{D_B}, H = \frac{\sigma B_o^{\ 2}}{\rho b}, Ec = \frac{u_w^2}{c_p\left(T_w - T_\infty\right)}, Rt = \frac{16\sigma_s T_\infty^3}{3kk^*}, TR = \frac{T_w}{T_\infty}, A = \frac{a}{c}, Bi = \frac{h}{k}\sqrt{\frac{\nu}{a}},$$
$$N_b = \frac{(\rho c)_p D_B\left(C_w - C_\infty\right)}{\rho c_p \nu},\ N_t = \frac{(\rho c)_p D_T\left(T_w - T_\infty\right)}{\rho c_p \nu T_\infty},\ \lambda = \lambda_1\sqrt{\frac{a}{\nu}},\ Q = \frac{Q_0}{a},\ Fm = \frac{C_b}{\rho\sqrt{k_0}}, \tag{15}$$
$$K = \frac{\nu}{ak_0},\ \xi = \sqrt{\frac{a}{\nu}}x\xi_1$$

$\Pr$ is Prandtl number, H is magnetic term, Le is Lewis number, λ and ξ are the slip and the critical shear rate parameters, Ec is the Eckert number, N_t and N_b respectively denote the thermophoresis and Brownian motion terms, Rt denoted the thermal radiation parameter, TR is the temperature ratio, Q is the heat generation term, and A is the stretching ratio parameter, Fm, K are the inertia coefficient parameter and the porosity parameter, while Bi denotes thermal Biot number.
The local drag force C_{fx}, local temperature gradient Nu_x, and local mass gradient Sh_x are presented as follows:

$$C_{fx} = \frac{\tau_w}{\rho u^2_{\ w}},\ Nu_x = \frac{xq_w}{k\left(T_w - T_\infty\right)},\ Sh_x = \frac{xq_m}{D_B\left(C_w - C_\infty\right)} \tag{16}$$

$$\tau_w = \left(\mu_B + \frac{p_y}{\sqrt{2\pi_c}}\right)\left(\frac{\partial u}{\partial y}\right)_{y=0},\ q_w = -k\left(\frac{\partial T}{\partial y}\right)_{y=0} + \left(q_r\right)_w,\ q_m = -D_B\left(\frac{\partial C}{\partial y}\right)_{y=0}$$

where shear stress is τ_w, the plate heat and mass flux q_w and q_m respectively. The dimensionless forms are

$$Re_x^{1/2} C_f = \left(1+\frac{1}{\beta}\right) f''(0),\ \frac{Nu}{Re_x^{1/2}} = -\left(1 + Rt\left(\left(TR-1\right)\theta(0)+1\right)^3\right)\theta'(0),\ \frac{Sh_x}{Re_x^{1/2}} = -\phi'(0) \tag{17}$$

$Re_x = \frac{xu_w}{v}$ Implies the Reynolds local number.

3. Numerical Solution

The Chebyshev spectra-collocation method was employed to obtain a numerical solution for the present non-linear system of derivative Eqs. (9)–(11) with boundary condition (12). In this technique, the functions $f(\eta) = \sum_{i=o}^{N} a_i T_i(\eta)$, $\theta(\xi) = \sum_{i=o}^{N} b_i T_i(\eta)$, and $\phi(\eta) = \sum_{i=o}^{N} c_i T_i(\eta)$ are approximated by the sum of the trial functions $T_n(\eta)$. The trial functions are taken in Chebyshev polynomials $T_n(\eta) = \cos\left(N\cos^{-1}\eta\right)$, $-1 \le \eta \le 1$, where a_n, b_n and c_n are unidentified constants to be determined. The range $[0,\infty]$ is the model domain which is then converted to $[-1,\ 1]$ to satisfied the trial functions, with the aid of $\eta = {}^{2\xi}\!/_{\xi_\infty} - 1$ where ξ_∞ denotes the boundary layer far stream. Now, to determine nonzero residual, introduce Eqn. (20) in Eqs. (9) – (11) for which the constant a_n, b_n and c_n are taken such that the residues are minimized all through the domain. Collocation integration method is employed for this study which is obtained as [25]:

$$\eta_i = \cos\left(\frac{i\pi}{Z}\right),\quad i = 0,1,2,3..Z \tag{18}$$

This produces schemes of algebraic equations in $3i+3$ together with $3i+3$ unknown constants a_j, b_j, and c_j to be determined, and Newton's iterative scheme is adopted for $j = 64$. Hence, boundary values problem algorithm is established in Mathematica software to have the computed results.

4. Discussion of Result

The influences of the emerging terms against the flow rate profiles $f'(\eta)$, temperature profiles $\theta(\eta)$, concentration profiles $\phi(\eta)$, plate frictional force $f''(\eta)$ and temperature gradient $\theta'(\eta)$ are discussed through graphs and Table1. Unless otherwise stated, in the framework of the present study the default values $Pr = 8.0,\ Le = 0.6,\ H = 0.5, K = 0.2, TR = 1.2,\ \lambda = \xi = 0.5,$ $N_b = 0.8, N_t = 0.3, Q = 0.1,\ Ec = 0.6,\ A = 0.2,\ \beta = 0.2, Fm = 0.2$ were use throughout the computation.

The effects of parameters H and A are display graphically in Fig. 2. It is clearly shown that the fluid flow rate decreases with an increasing value of H which is physically reasonable in the present of inclined magnetic field. This stimulated an opposing force known as Lorentz force that is analogous to drag frictional force which resists the free flow of the fluid. Meanwhile, an upsurge in the velocity ratio values A enhanced the velocity profiles due internally generated heat that damped the molecular bonding of the fluid particles. In Fig. 3, it is obtained that increasing the porosity permeability term K and Froude number Fm leads to overall damps in the velocity of the fluid particle along the bounded flow stream. The flow parameter sensitivity is because of the thinner in the momentum boundary layer that helps in keeping the fluid temperature throughout the flow region. The impact of slip and the critical shear rate parameters are portrayed in Fig. 4, and it is revealed that the flowing fluid diminishes with the enhancement of slip velocity term. The velocity boundary layer viscosity along with the unconditional value of velocity rises with an increased critical shear rate parameter. Fig.5 exemplifies the Casson parameter β influence on the non-dimensional velocity. It is clearly noticed that an upsurge in the values of β leads to a shrinkage in both velocity profiles and the corresponding boundary layer viscidness. The fluid viscoelastic property is enhanced to restrict free liquid particles movement, as such; the flow velocity regime is damped.

The temperature solution profiles across the viscosity of the boundary layer at various values of dimensionless Prandtl number $\Pr$ and Eckert number Ec are depicted in Fig. 6. As noticed, an increase in $\Pr$ numbers decrease the boundary layer thickness, because lager Prandtl number describes feebler heat diffusivity which causes thinner thermal boundary film. Meanwhile, temperature distribution is enriched with rising Eckert number. Eckert number corresponding to heat dissipation and dispersion is a system, in this view, heat propagation in encouraged as a result of strong particle collision and lower fluid mass molecular bonding. As such, the heat field is boosted to improve heat conductivity and diffusion. The Influence of thermal radiation and temperature ratio are shown in Fig. 7. It shows an increasing behavior of $\theta(\eta)$ for higher heat radiation values Rt and the temperature ratio TR parameters on temperature profiles. This is because the temperature boundary film increases with a rise in both heat radiation and temperature ratio. This observation and outcome agreed well with other published articles, as reported, the terms enhances internal production of heat that inspires heat transfer and emboldens increasing temperature field.

The impact of velocity ratio A and heat generation Q on the temperature field is presented in Fig. 8. The plots show that an increase in A results to decrease in the temperature profiles because the chemical bonding is stimulated close to the moving plate. But far away for the laminar steady flow, a uniform temperature distribution is obtained towards the boundless stream. However, converse behaviour for the heat generation is detected because a rise in the heat source raises the heat production that leads to an enhancing temperature profile. The plot of $\theta(\eta)$ versus η demonstrating the influence of Casson term β and Biot number Bi on the heat transfer is separately represented in Fig. 9. An increase in both β and Bi enhanced the temperature profiles because of the stimulation of internal heating that inspires the heat transfer in the flow medium. The parameters encourage species reaction that lead to molecular diffusion which thereby augments temperature distributions along the flow region.

Fig. 10 depicts the response of temperature field to increase values of thermophoresis term Nt and Brownian movement term Nb. The temperature profiles increase with an increasing values of Nt and Nb. The Brownian movement generates fluid molecular micro-mixing that resulted in the augmentation of thermal nanofluid conductivity. A rise in the thermal nanofluid convection and conductivity influence leads to increasing temperature function. This outcome is significant to the thermal sciences and industrial engineering in enhancing machine efficiency and productivity. Fig. 11 shows the effects Fm and β on the mass species transfer profiles. The mass boundary layer viscidness reduced as the value of Fm increases while an augmentation in the Casson material term β enhanced the chemical species reaction profiles.

The plot representing the bodily quantities of curiosity, the plate surface coefficient of skin friction, local Nusselt number and mass gradient which have enormous engineering usages are related to the values of $\left(1+\frac{1}{\beta}\right)f''(0), -\theta'(0) \text{and} -\phi'(0)$ correspondingly. In Fig. 12, the computed values of $\left(1+\frac{1}{\beta}\right)f''(0)$ against H and ξ are presented and it noticed that the magnitude of wall skin friction increase with an increase in the values of Fm and K. In figure 13, decrease in Nusselt number can be clearly viewed with an increase in Brownian motion while increase in Prandtl number enhanced the Nusselt number. Sherwood number increases with large value of Lewis number Le, while it decreases with an increase in Brownian motion parameter in figure 14.

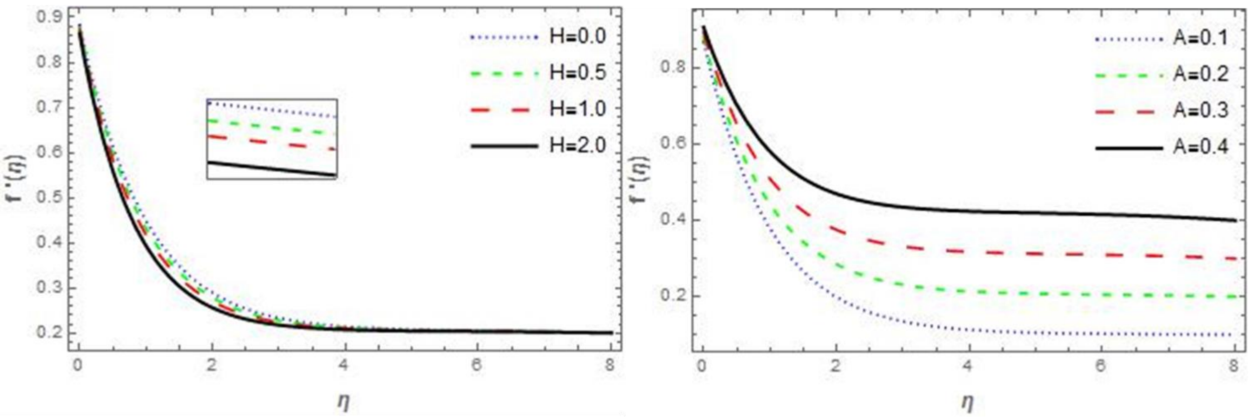

Fig.2 . Influence of H and A on $f'(\eta)$

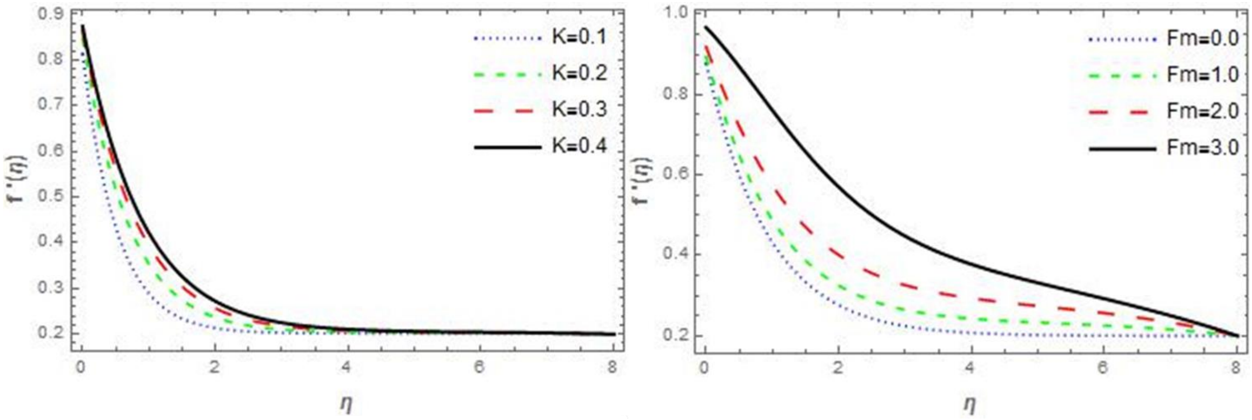

Fig. 3. Influence of K and Fm on $f'(\eta)$

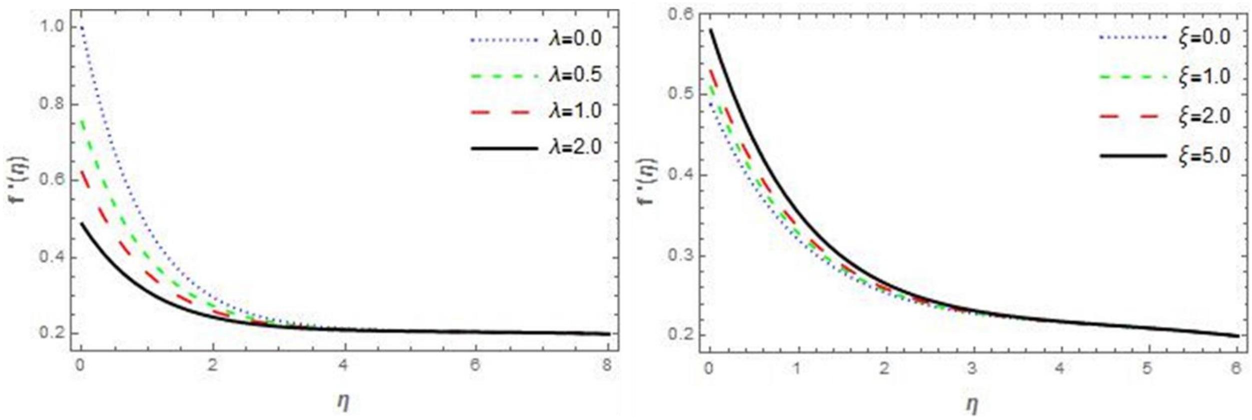

Fig. 4. Influence of λ and ξ on $f'(\eta)$

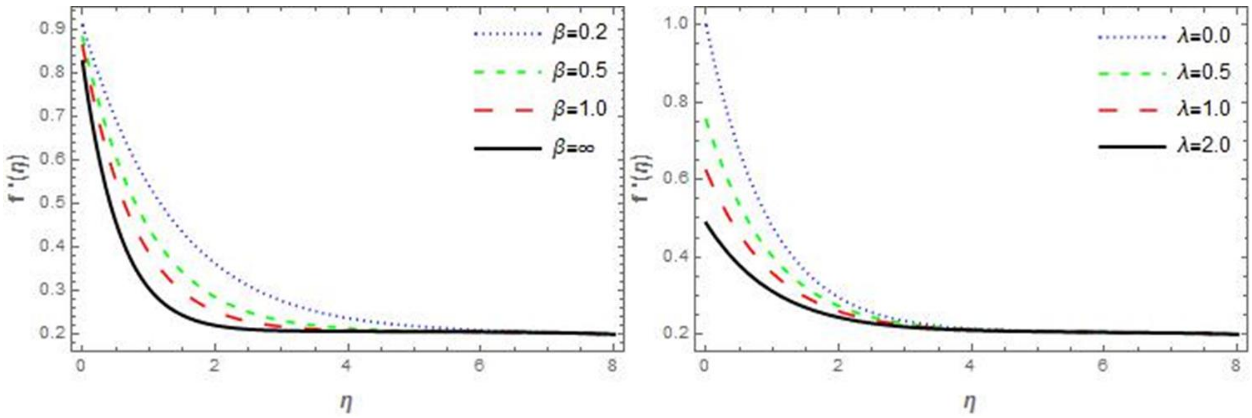

Fig. 5. Influence of β on $f'(\eta)$

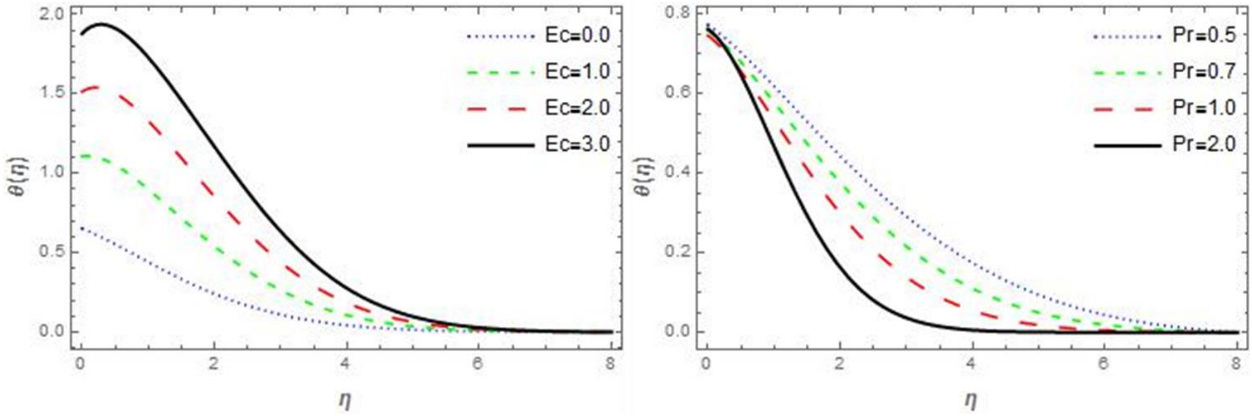

Fig. 6. Influence of Ec and $\Pr$ on $\theta(\eta)$

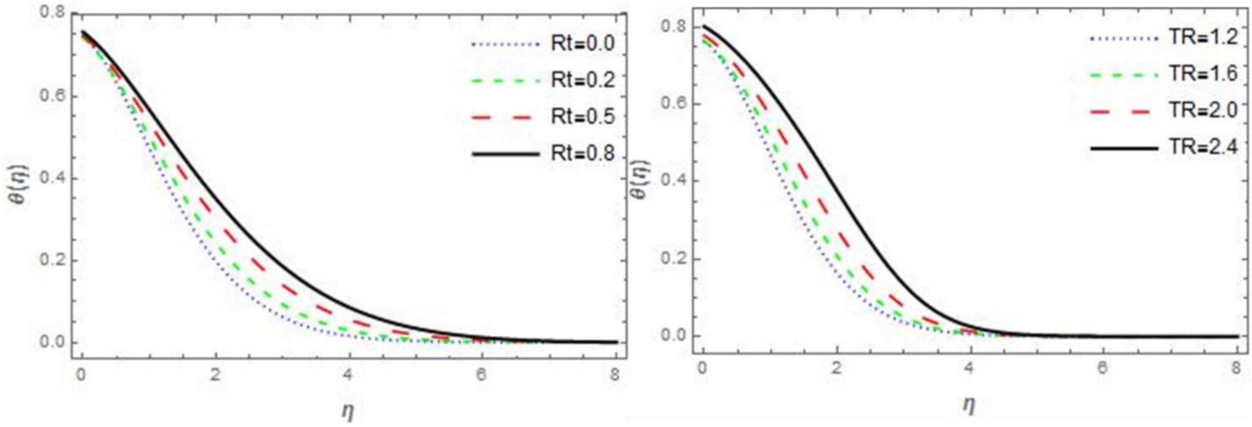

Fig. 7. Influence of Rt and TR on $\theta(\eta)$

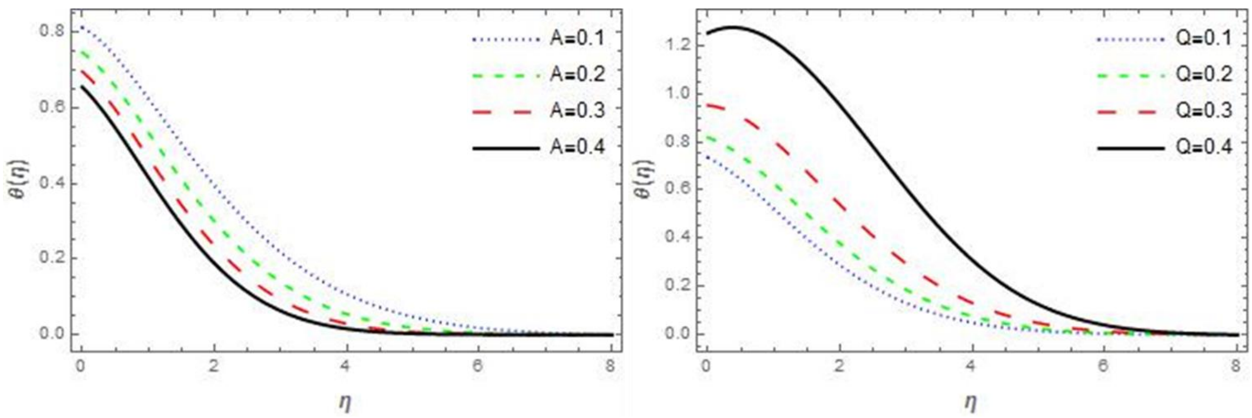

Fig. 8. Influence of A and Q on $\theta(\eta)$

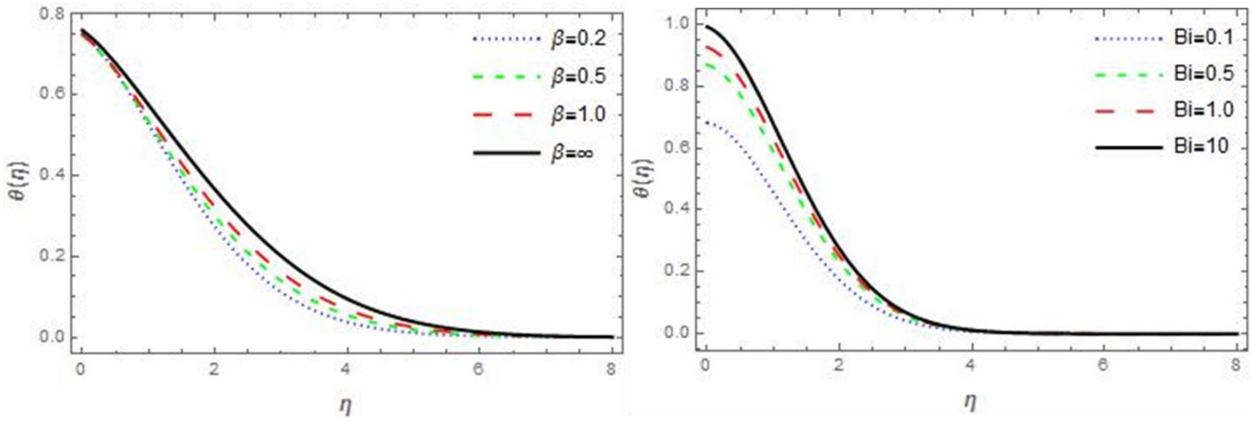

Fig. 9. Influence of β and Bi on $\theta(\eta)$

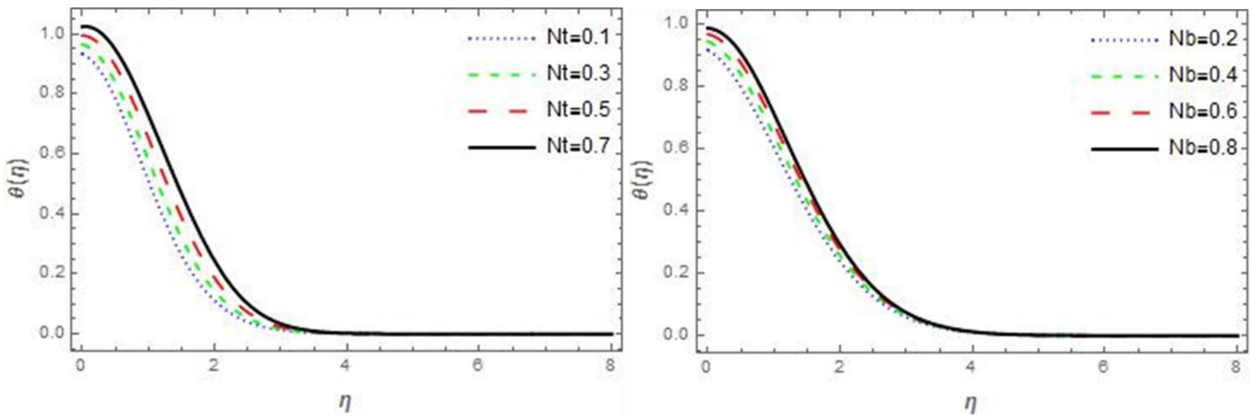

Fig. 10. Influence of Nt and Nb on $\theta(\eta)$

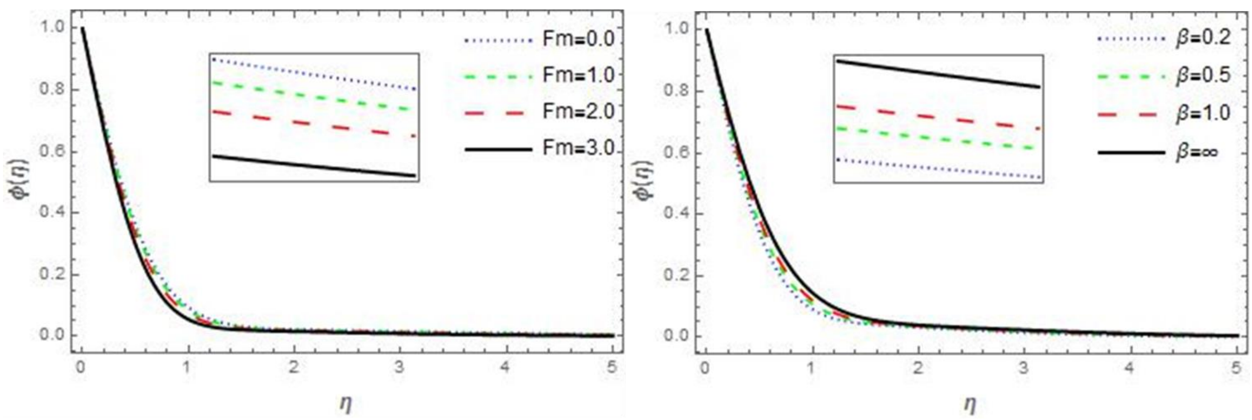

Fig. 11. Influence of Fm and β on $\phi(\eta)$

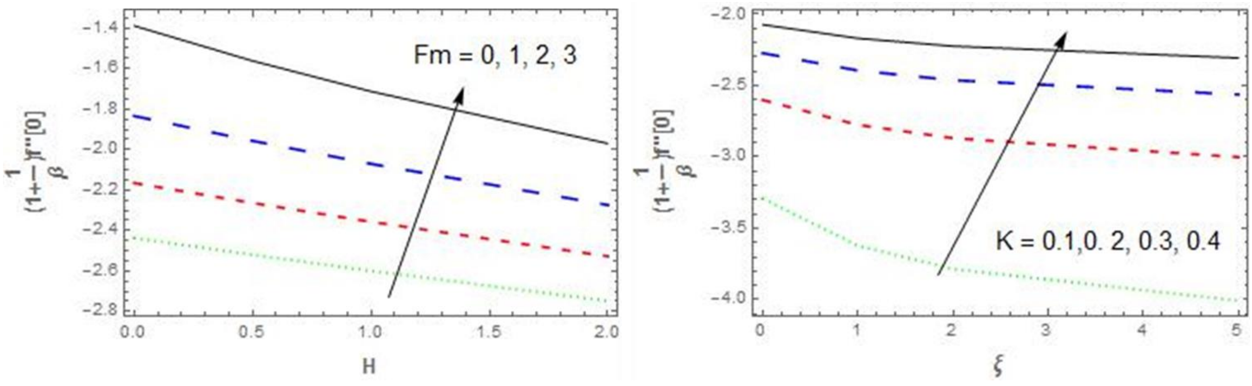

Fig. 12. Influence of H, Fm, K and ξ on $\left(1+\dfrac{1}{\beta}\right) f''(\eta)$

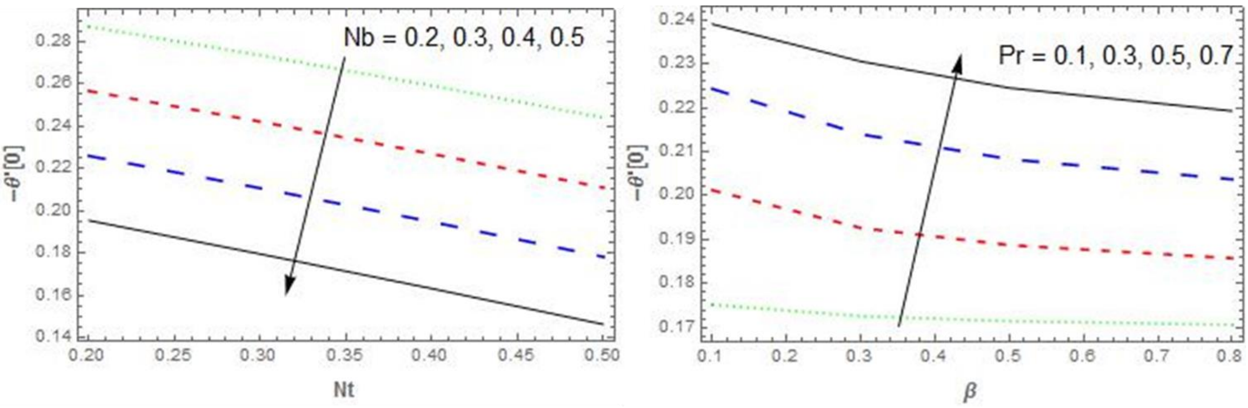

Fig. 13. Influence of $Nb, Nt, \Pr$ and β on $-\theta'(\eta)$

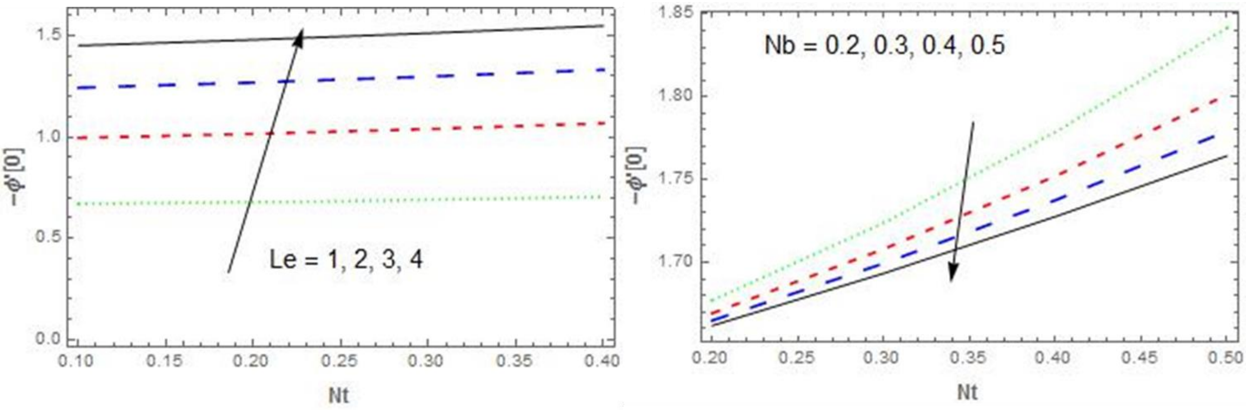

Fig. 14. Influence of $Nb, Nt,$ and Le on $-\phi'(\eta)$

Table 1
Comparison of numerical data of $-\theta'(0)$ for varying values of P_r with previous existing results when $Le = 10, \beta = K \to \infty, B_i = 1{,}000 H = Fm = Rt = Ec = N_t = N_b = A = \lambda = 0$

	Hussain et al. [26]	Mahmood et al. [27]	Present result
Pr	$-\theta'(0)$	$-\theta'(0)$	$-\theta'(0)$
0.07	0.06637	0.0663	0.06582730
0.02	0.16913	0.1691	0.16759351
0.70	0.45395	0.4539	0.45086370
2.00	0.91132	0.9113	0.91052766

Table 2
Numerical data for skin friction coefficient, reduced Nusselt number and Sherwood number for different values of β, H, $\Pr$, N_t, N_b, δ, E, Me, Q

β	H	$\Pr$	N_t	N_b	λ	K	Rt	Q	$-\left(1+\frac{1}{\beta}\right)f''$	$-\left(\begin{array}{c}1+Rt\\ \left(\frac{(TR-1)}{\theta+1}\right)^3\end{array}\right)\theta'$	$-\phi'$
0.5	0.5	0.8	0.3	0.8	2.0	0.2	0.2	0.1	-0.683211	0.269483	1.54005
1.0									-0.811333	0.266360	1.48708
∞									-1.07769	0.257137	1.38668
	0.0								-1.93565	0.289908	1.54705
	0.5								-2.04963	0.269483	1.54005
	1.0								-2.15536	0.250881	1.53358
		0.5							-2.04963	0.238611	1.52756
		0.7							-2.04963	0.254079	1.53170
		1.0							-2.04963	0.269483	1.54005
			0.1						-1.98233	0.296152	1.52966
			0.3						-1.98233	0.286409	1.53866
			0.5						-1.98233	0.276557	1.55036
				0.2					-1.98233	0.301307	1.54419
				0.4					-1.98233	0.281496	1.54418
				0.6					-1.98233	0.262239	1.54385
					0.0				-2.35272	0.272818	1.64879
					0.5				-1.59744	0.284877	1.42962
					1.0				-1.20155	0.291364	1.30417
						0.1			-3.48932	0.152174	1.40659
						0.2			-2.70337	0.215553	1.47487
						0.3			-2.34311	0.247739	1.50869
							0.0		-2.34311	0.109882	1.55360
							0.2		-2.34311	0.114060	1.53216
							0.5		-2.34311	0.113718	1.51694
								0.1	-2.34311	0.201216	1.51694
								0.2	-2.34311	0.118087	1.55070
								0.3	-2.34311	-0.0374619	1.60539

5. Conclusion

Influence of nonlinear thermal radiation on a stagnation point of an aligned MHD non-Newtonian Casson nanofluid flow with Thompson and Troian slip boundary condition is examined in this research. The stretching plate is assumed to exchange heat with the ambient temperature. The final remarks of the present analysis are highlighted as follows:

- the temperature boundary layer thickness increase with large values of thermal radiation and temperature ratio;
- It is evident from our findings that the concentration profile is rapidly compressed by increase in Froude number Fm and Casson parameter β;
- Heat transfer rate continuously decreases for increasing trend of Prandtl number Pr;
- With the increase in the value of Hartmann H, Froude number Fm, and porosity permeability parameter K, the velocity boundary layer thickness and the absolute value of velocity decrease;
- The fluid velocity increases with an escalation in the value of ξ.

Therefore, this research will assist the thermal science and the industrial engineering in improving the efficiency of their based fluids and engines/machines productivity. As such, the study can be extended to flow in an annular cylinder medium with Arrhenius chemical kinetics.

References

[1] Gireesha, B. J., B. M. Shankaralingappa, B. C. Prasannakumar, and B. Nagaraja. "MHD flow and melting heat transfer of dusty Casson fluid over a stretching sheet with Cattaneo–Christov heat flux model." *International Journal of Ambient Energy* (2020): 1-9.

[2] Mabood, Fazle, T. A. Yusuf, and I. E. Sarris. "Entropy generation and irreversibility analysis on free convective unsteady MHD Casson fluid flow over a stretching sheet with Soret/Dufour in porous media." *Special Topics & Reviews in Porous Media: An International Journal* 11, no. 6 (2020).

[3] Kirubhashankar, C. K., S. Vaithyasubramanian, Y. Immanuel, and P. Muniappan. "Thermal Effects on Magneto Hydrodynamic Casson Liquid Stream Between Electrically Conducting Plates." *International Journal of Innovative Technology and Exploring Engineering (IJITEE)* 9, no. 4 (2020): 213-217.

[4] Reddy, P. Bala Anki, B. Mallikarjuna, and K. Madhu Sudhan Reddy. "Slip effect on heat and mass transfer in Casson fluid with Cattaneo–Christove heat flux model." *Frontiers in heat and mass transfer* 5 (2018)

[5] El-Aziz, Abd, and Ahmed A. Afify. "Influences of slip velocity and induced magnetic field on MHD stagnation-point flow and heat transfer of Casson fluid over a stretching sheet." *Mathematical Problems in Engineering* 2018 (2018).

[6] Khan, Zeeshan, Haroon Ur Rasheed, Saeed Islam, Sahib Noor, Waris Khan, Tariq Abbas, Ilyas Khan, Seifedine Kadry, Yunyoung Nam, and Kottakkaran Sooppy Nisar. "Impact of magnetohydrodynamics on stagnation point slip flow due to nonlinearly propagating sheet with nonuniform thermal reservoir." *Mathematical Problems in Engineering* 2020 (2020).

[7] Ahmad .K, Wahid .Z and Hanouf .Z, :(2017) ''Stagnation point flow of Casson fluid over exponentially stretching sheet with variable thermal conductivity and Newtonian heating,'' International Journal of Advances in Mechanical Engineering, vol.4, no. 2, pp. 2394-2827.

[8] Ullah, Imran, Tawfeeq Abdullah Alkanhal, Sharidan Shafie, Kottakkaran Sooppy Nisar, Ilyas Khan, and Oluwole Daniel Makinde. "MHD slip flow of Casson fluid along a nonlinear permeable stretching cylinder saturated in a porous medium with chemical reaction, viscous dissipation, and heat generation/absorption." *Symmetry* 11, no. 4 (2019): 531.

[9] Lund, Liaquat Ali, Zurni Omar, Ilyas Khan, Dumitru Baleanu, and Kottakkaran Sooppy Nisar. "Dual similarity solutions of MHD stagnation point flow of Casson fluid with effect of thermal radiation and viscous dissipation: stability analysis." *Scientific reports* 10, no. 1 (2020): 1-13.

[10] Ghosh, Sudipta, and Swati Mukhopadhyay. "MHD slip flow and heat transfer of Casson nanofluid over an exponentially stretching permeable sheet." *International Journal of Automotive & Mechanical Engineering* 14, no. 4 (2017).

[11] Raju, C. S. K., and N. Sandeep. "Nonlinear radiative magnetohydrodynamic Falkner-Skan flow of Casson fluid over a wedge." *Alexandria Engineering Journal* 55, no. 3 (2016): 2045-2054.

[12] Uddin, Iftikhar, Rizwan Akhtar, Zhu Zhiyu, Saeed Islam, Muhammad Shoaib, and Muhammad Asif Zahoor Raja. "Numerical treatment for Darcy-Forchheimer flow of Sisko nanomaterial with nonlinear thermal radiation by lobatto IIIA technique." *Mathematical Problems in Engineering* 2019 (2019).

[13] Oyelakin, Ibukun Sarah, Sabyasachi Mondal, and Precious Sibanda. "Unsteady Casson nanofluid flow over a stretching sheet with thermal radiation, convective and slip boundary conditions." *Alexandria engineering journal* 55, no. 2 (2016): 1025-1035.

[14] Murugesan, Thiagarajan, and M. Dinesh Kumar. "Effects of thermal radiation and heat generation on hydromagnetic flow of nanofluid over an exponentially stretching sheet in a porous medium with viscous dissipation." *World Scientific News* 128, no. 2 (2019): 130-147.

[15] Daniel, Yahaya Shagaiya, Zainal Abdul Aziz, Zuhaila Ismail, and Faisal Salah. "Thermal radiation on unsteady electrical MHD flow of nanofluid over stretching sheet with chemical reaction." *Journal of King Saud University-Science* 31, no. 4 (2019): 804-812.

[16] Jawad, Raza, Mushayydha Farooq, and B. Mahanthesh FatehMebarek-oudina. "Multiple slip effects on MHD non-Newtonian nanofluid flow over a nonlinear permeable elongated sheet." *Multidiscipline Modeling in Materials and Structures* 15, no. 5 (2019): 913-931.

[17] Hayat, T., M. Ijaz Khan, Sumaira Qayyum, A. Alsaedi, and M. Imran Khan. "New thermodynamics of entropy generation minimization with nonlinear thermal radiation and nanomaterials." *Physics Letters A* 382, no. 11 (2018): 749-760.

[18] Mohyud-Din, Syed Tauseef, Umar Khan, Naveed Ahmed, Ilyas Khan, T. Abdeljawad, and Kottakkaran Sooppy Nisar. "Thermal Transport Investigation in Magneto-Radiative GO-MoS2/H2O-C2H6O2 Hybrid Nanofluid Subject to Cattaneo–Christov Model." *Molecules* 25, no. 11 (2020): 2592.

[19] Khan, Umair, Shafiq Ahmad, Arsalan Hayyat, Ilyas Khan, Kottakkaran Sooppy Nisar, and Dumitru Baleanu. "On the Cattaneo–Christov Heat Flux Model and OHAM analysis for three different types of nanofluids." *Applied Sciences* 10, no. 3 (2020): 886.

[20] EswaraRao, M., and S. Sreenadh. "MHD flow of a Casson fluid over an exponentially inclined permeable stretching surface with thermal radiation, viscous dissipation and chemical reaction." *Global Journal of Pure and Applied Mathematics* 13, no. 10 (2017): 7529-7548.

[21] Kumar, Rakesh, Ravinder Kumar, M. Sheikholeslami, and Ali J. Chamkha. "Irreversibility analysis of the three dimensional flow of carbon nanotubes due to nonlinear thermal radiation and quartic chemical reactions." *Journal of Molecular Liquids* 274 (2019): 379-392.

[22] Albeshri, Badr Ali Bzya, Nazrul Islam, Ahmad Yahya Bokhary, and Amjad Ali Pasha. "Hydrodynamic Analysis of Laminar Mixed Convective Flow of Ag-TiO2-Water Hybrid Nanofluid in a Horizontal Annulus." *CFD Letters* 13, no. 7 (2021): 47-57.

[23] Halim, Nur Fazlin Che, and Nor Azwadi Che Sidik. "Mixing Chamber for Preparation of Nanorefrigerant." *Journal of Advanced Research in Applied Sciences and Engineering Technology* 21, no. 1 (2020): 32-40.

[24] Jahan, Sultana, M. Ferdows, M. D. Shamshuddin, and Khairy Zaimi. "Effects of Solar Radiation and Viscous Dissipation on Mixed Convective Non-Isothermal Hybrid Nanofluid over Moving Thin Needle." *Journal of Advanced Research in Micro and Nano Engineering* 3: 1-11.

[25] Usman, Auwalu Hamisu, Sadiya Ali Rano, and Poom Kumam. "Activity of Viscoelastic Nanofluid Film Sprayed on a Stretching Cylinder with Arrhenius Activation Energy and Entropy Generation." *Journal of Advanced Research in Micro and Nano Engineering* 3, no. 1 (2021): 12-24.

[26] Vijayaragavan, R., and S. Karthikeyan. "Hall current effect on chemically reacting MHD Casson fluid flow with dufour effect and thermal radiation." *Asian J Appl Sci Technol* 2, no. 2 (2018): 228-245.

[27] Noura S.A. (2017), Heat generation and radiation effects on MHD Casson fluid flow over a stretching surface through porous medium, European journal of Advances in Engineering and Technology, 4(11): 850-857.

[28] Haq, Sami Ul, Syed Inayat Ali Shah, Kottakkaran Sooppy Nisar, Saeed Ullah Jan, and Ilyas Khan. "Convection heat mass transfer and MHD flow over a vertical plate with chemical reaction, arbitrary shear stress and exponential heating." *Scientific Reports* 11, no. 1 (2021): 1-11.

[29] Sun, Ya-Song, Jing Ma, and Ben-Wen Li. "Chebyshev collocation spectral method for three-dimensional transient coupled radiative–conductive heat transfer." (2012): 092701.

[30] Hussain, T., S. A. Shehzad, A. Alsaedi, T. Hayat, and M. J. J. O. C. S. U. Ramzan. "Flow of Casson nanofluid with viscous dissipation and convective conditions: a mathematical model." *Journal of Central South University* 22, no. 3 (2015): 1132-1140.

[31] Mahmood, M., S. Asghar, and M. A. Hossain. "Transient mixed convection flow arising due to thermal and mass diffusion over porous sensor surface inside squeezing horizontal channel." *Applied Mathematics and Mechanics* 34, no. 1 (2013): 97-112.